Electronic Supplementary Material (ESI) for Environmental Science: Nano.

Supporting Information

Fluorogenic hyaluronan nanogels for detection of micro- and nanoplastics in water

Matteo Cingolani, Enrico Rampazzo, Nelsi Zaccheroni, Damiano Genovese* and Luca Prodi*

List of Contents

1.1 HA-RB photophysical characterization

To evaluate the photophysical properties of the HA-RB probe we acquired absorbance and emission for calculation of photoluminescence quantum yield (PLQY) and dynamic light scattering (DLS) measure for average size information. Rhodamine B solution in ethanol was used as a reference (PLQY=0.65). HA-RB spectra were recorded both in ethanol and water

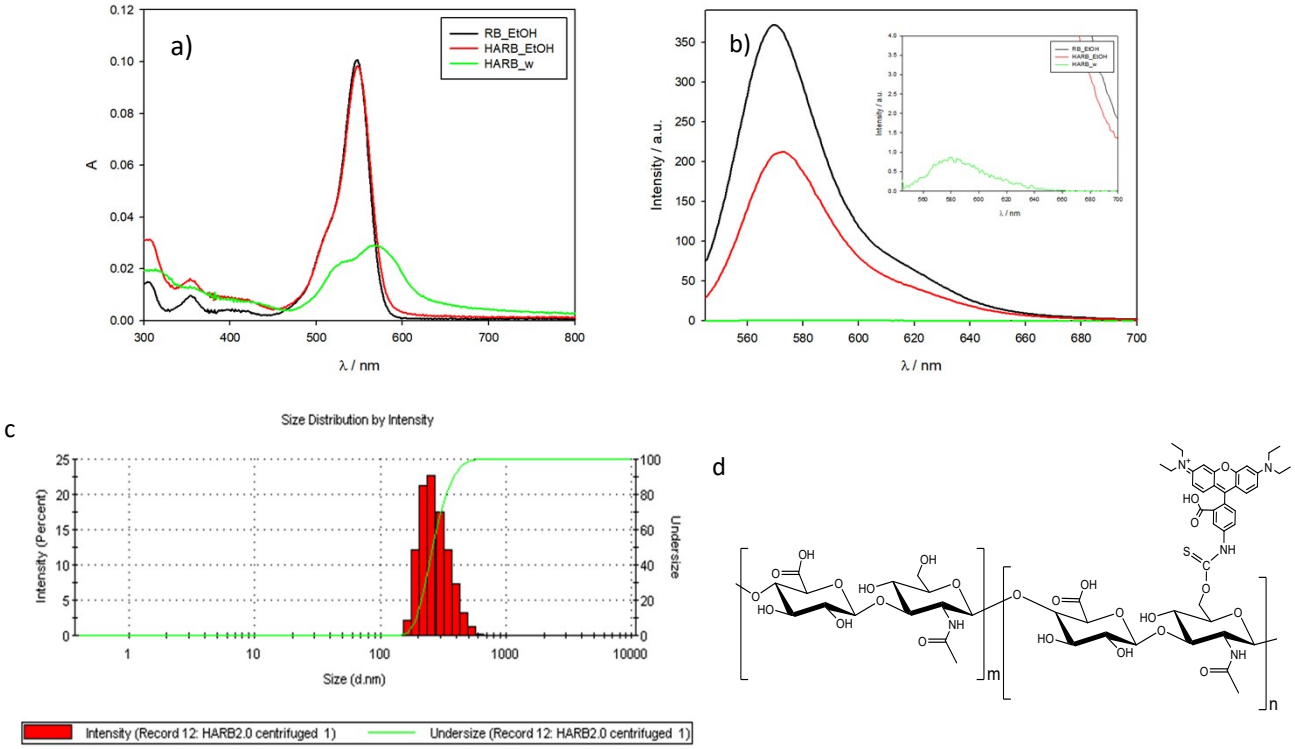

Figure S1 *- Absorbance (a) and emission spectra (b, λ_{exc} = 530 nm) of the reference dye Rhodamine B in ethanol (RB_EtOH) and of HA-RB in ethanol and milliQ water solution (HA-RB_EtOH and HA-RB-w, respectively, both at [HA-RB] = 38 nM). Figure c shows the dynamic light scattering measurement of the solution of HA-RB (dH = 320 nm, polydispersity index PdI = 0.287). d) Molecular structure of rhodamine functionalized hyaluronic acid (m/n ~ 60).*

The calculated photoluminescence quantum yield for the probe in the two different solvent is 0.39 for HA-RB in ethanol and $4.23*10^{-3}$ for HA-RB in Milli-Q water.

The same solutions were used to register the fluorescence lifetime decay with TCSPC experiment (Table S1)

Table S1 - Fluorescence lifetimes of RB dye in ethanol, of HA-RB in ethanol and in water

Sample	τ (ns)	χ^2
RB (ethanol)	2.88	1.006
HA-RB (ethanol)	2.79	0.903
HA-RB (water)	1.80	1.035

The probe effective degree of functionalization was evaluated by UV-vis analysis measuring the absorbance of Rhodamine B in ethanol solution at known concentration of HA-RB. Since the two spectra feature similar properties as the free dye we can use with a reasonable assumption the molar extinction coefficient of the free Rhodamine B in ethanol (106000 $cm^{-1}M^{-1}$). The HA-RB calculated degree of functionalization is 1.7 % (ca. 1 dye molecule every 60 monomers of hyaluronic acid).

1.2 Hydrogel medium for microscope sample images acquisition- photophysical probe changes evaluation.

On the microscope slide, most of the microplastic samples tend to accumulate in a specific region of the drop of the solution they are dispersed in (drop surface and borders). In order to have a homogenous dispersed sample in the drop we used a more viscous medium that does not interfere with the photophysical properties of HA-RB.

We tested the probe HA-RB (~ 10^{-5} M) in Glycerol (Gly) and hyaluronan hydrogel (HAgel, 16mg/mL native HA 200-600 KDa in water) monitoring its emission signal at 580 nm through time for the system to equilibrate. As reference we used the emission spectra of Rhodamine B (RB) and HA-RB in Milli-Q water (figure S2)

The graph in figure S2 shows that the probe has a significant enhancement of emission in glycerol compared to the native hyaluronan which was selected since it does not interfere with the photophysical properties of HA-RB. Absorption and emission spectra are slightly red-shifted in glycerol due to solvatochromism.

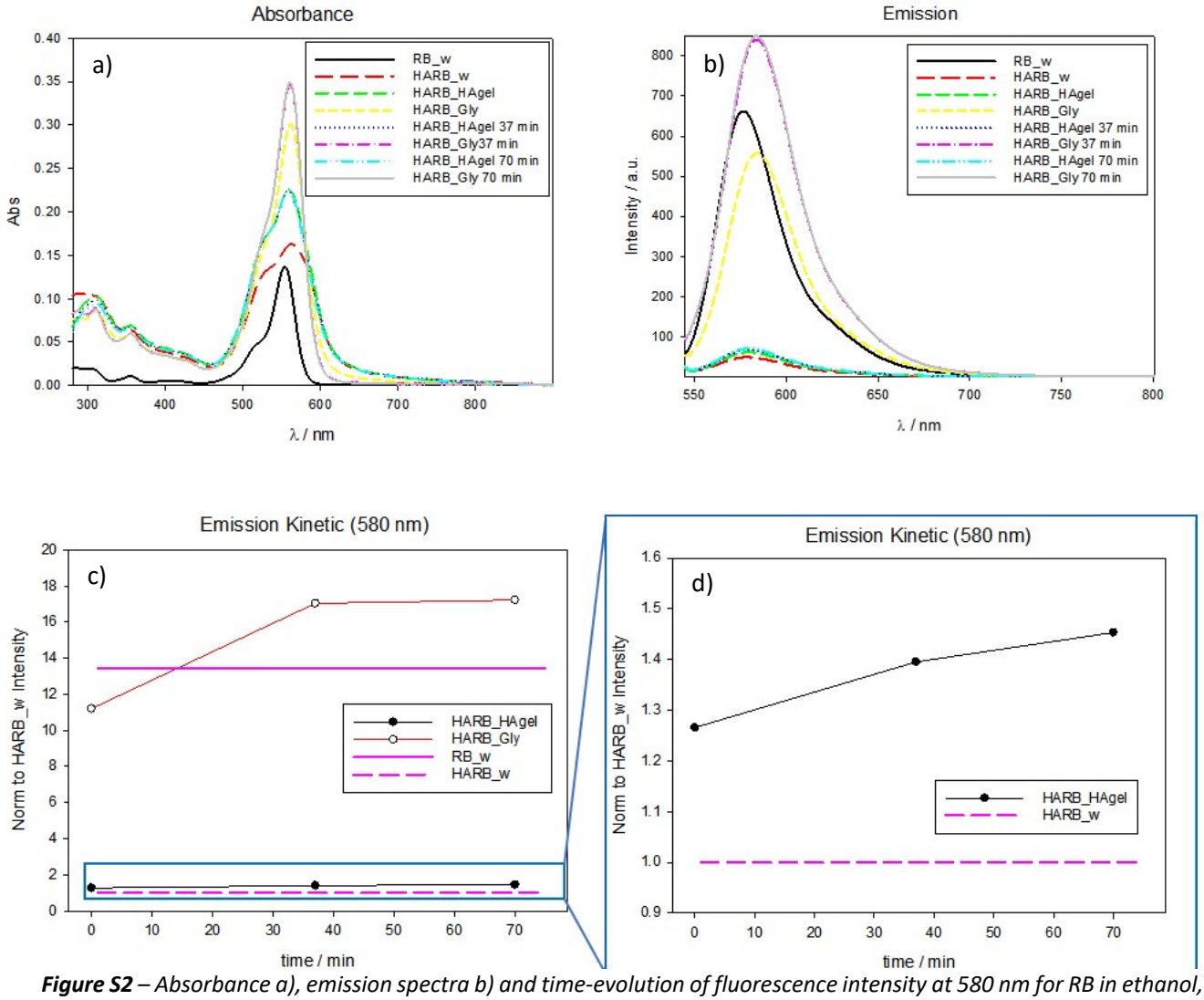

Figure S2 *– Absorbance a), emission spectra b) and time-evolution of fluorescence intensity at 580 nm for RB in ethanol, HA-RB in ethanol and HA-RB in water c) and d). The fluorescence emission signal was normalized to HA-RB_w value.*

2 Confocal microscopy acquisition and image analysis

2.1 MNP@HA-RB: dependence of lifetime on [HA-RB] concentration.

To evaluate the dependence of lifetime on probe concentration adsorbed on the microplastic surface we incubated 3 samples of PVC with 0.6 nM, 5.6 nM and 1.1 µM HA-RB (concentration of polymer chains). After the purification steps, the sample was dispersed in the native hyaluronan hydrogel and we acquired confocal and FLIM microscope images (figure S3) with the same optical parameters.

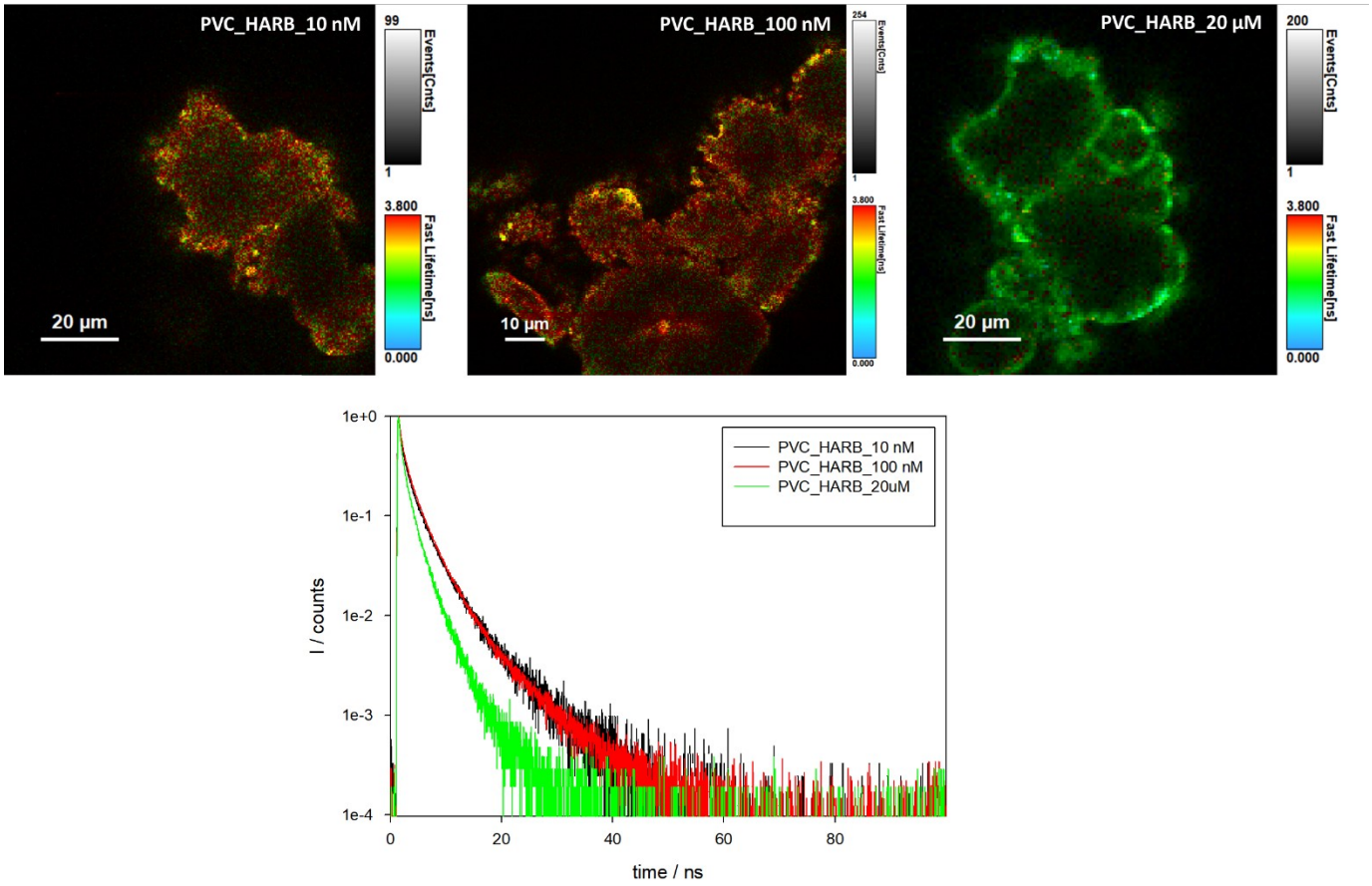

***Figure S3**- FLIM acquisitions indicate that 0.6 nM and 5.6 nM concentration of the probe lead to the same lifetime decay showing that in this concentration range the photophysical properties of the HA-RB remain unchanged. The higher concentration 1.1 µM instead show a marked decrease in the lifetime decay due to the accumulation of HA-RB on the microplastic surface favouring the self-quenching of RB moieties.*

2.2 Nile Red + microplastic: false positive for small fragment recognition

Nile Red is a common fluorescent dye for fluorescent staining of microplastics. Samples of microplastic have been incubated in water solution of Nile Red in the same way of HA-RB probe. The confocal images reveal that Nile Red adsorbs onto microplastics surface leading to fluorescence intensity comparable to MNPs stained with HA-RB. Yet, the images also show the presence of NR aggregates with typical "needle-like" morphology – providing "false positive" fluorescent objects – that can only be discriminated via FLIM analysis (figure S4c-d).

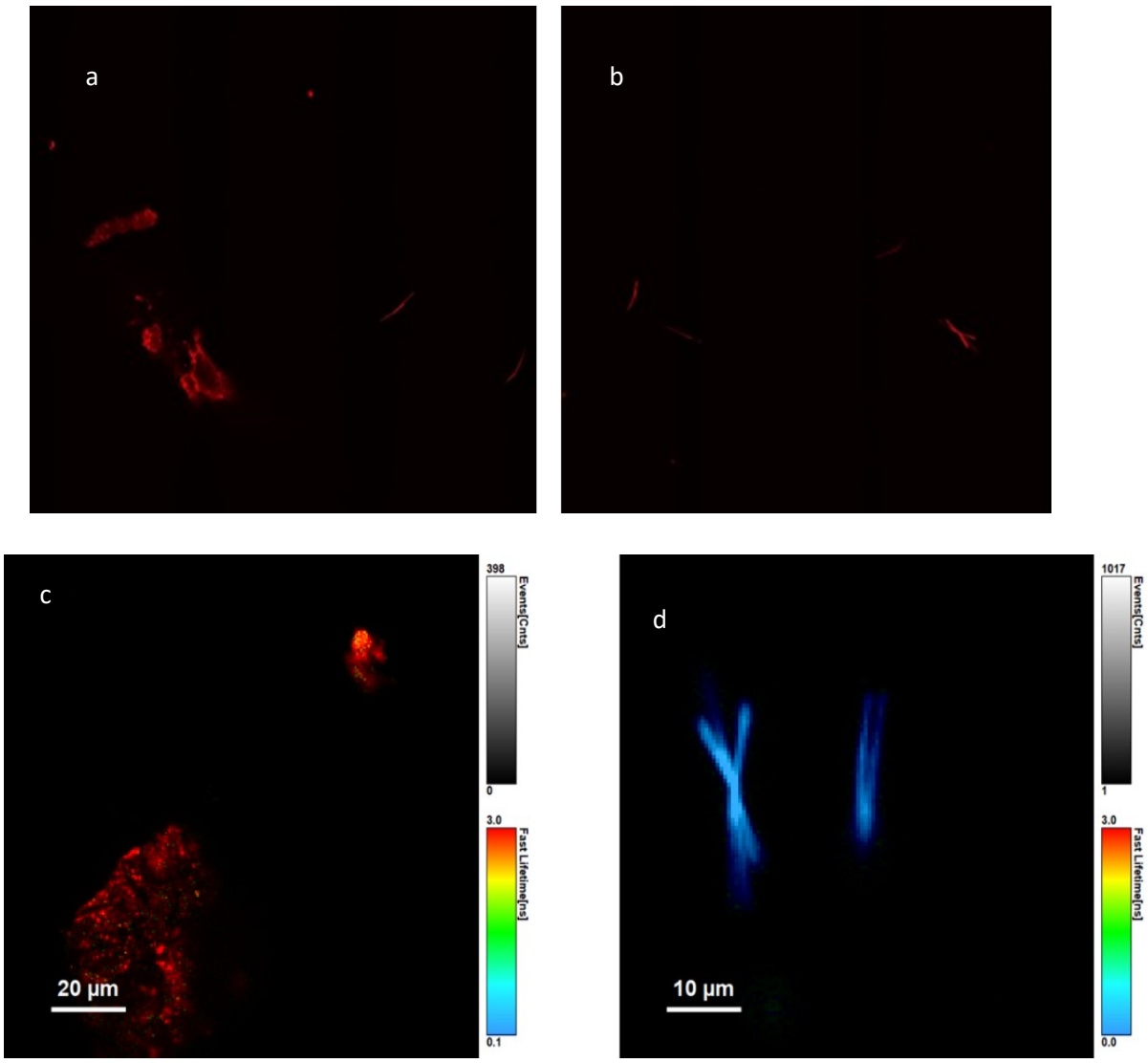

Figure S4*- In figures a) and b) are reported two mosaic acquisitions of PMMA+NR where both microplastics fragment and needle-like NR aggregates are present. FLIM images reported in c) and d) show clearly different lifetimes of NR when on PMMA surface respect to its own aggregates.*

2.3 Microplastic Confocal and FLIM acquisitions

Confocal images were acquired with the same optical parameters for MNPs incubated with 170nM and 5.6 nM HA-RB. Multi-frame mosaic acquisitions of 10x10 images were captured in the range of 5-50 µm height from the glass slide surface.

FLIM images were captured right after the confocal images with a 405 nm pulsed laser source and an

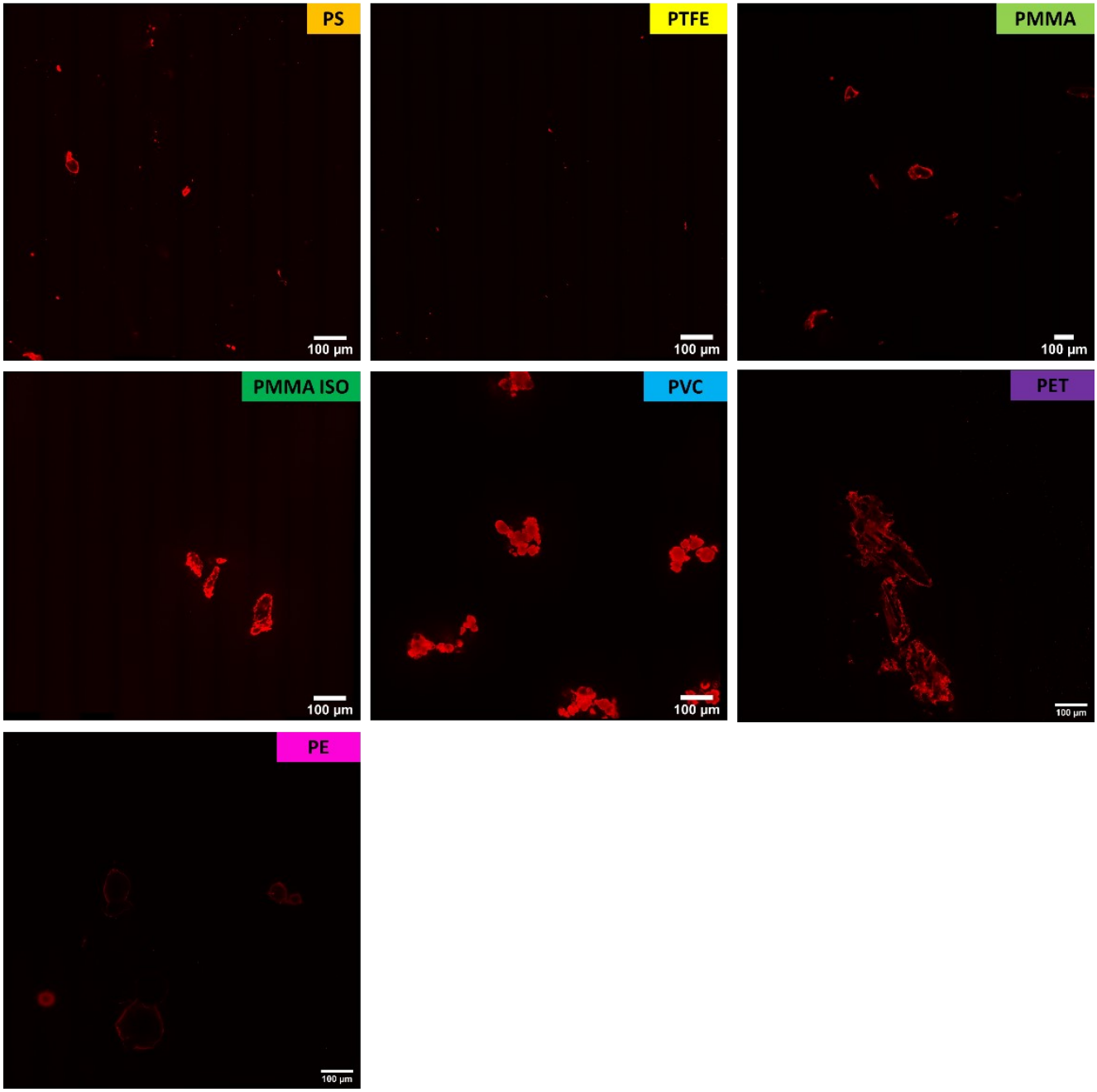

Figure S5 *–Confocal images of microplastic samples incubated with 170 nM HA-RB. Acquisition parameters and LUTs are the same for all images.*

emission cut-off filter at 560 nm. The acquisition lasted 60 seconds for each sample to ensure sufficient photon accumulation (peak counts in fitted areas > 10^3).

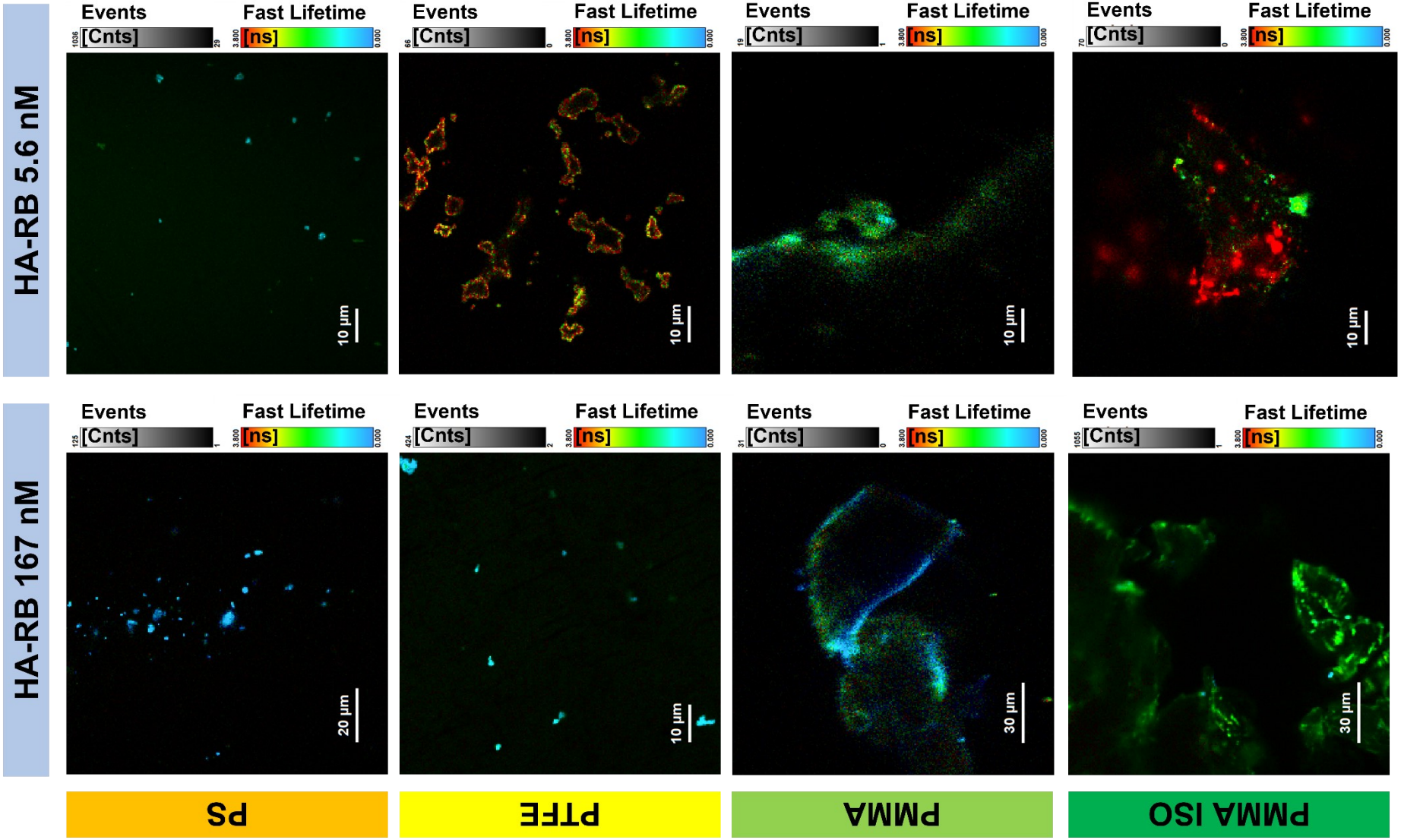
HA-RB 5.6 nM
HA-RB 167 nM
Events
[Cnts]
Fast Lifetime
[ns]
10 µm
20 µm
30 µm
PS
PTFE
PMMA
PMMA ISO

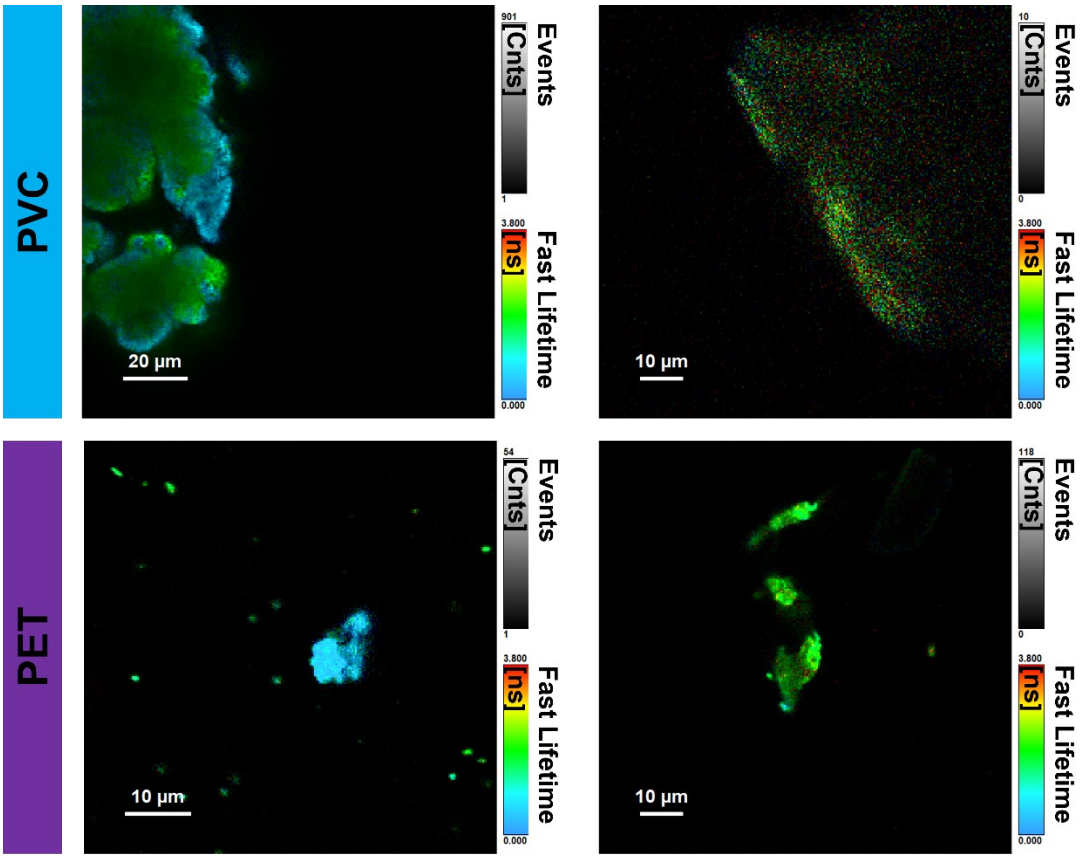

Figure S6 *- FLIM images of MNPs sample at two concentrations of HA-RB (left images [HA-RB] = 170 nM, right images [HA-RB] = 5.6 nM.*

2.4 Image analysis

FLIM

FLIM images were analysed with SymPhoTime 64, PicoQuant GmbH. For each image we selected different regions of interest (ROIs) relative to the microplastic surface and each associated lifetime decay was fitted with "n-Exponential Reconvolution Fit" model. In all cases we use either 2 or 3 exponentials to obtain satisfactory fittings, probably due to the heterogeneous nature of the RB dyes in the HA-RB nanogels and on the non-homogeneous unquenching upon interaction with MNPs surfaces. Therefore, for each sample, we took the τ_Av_Int of the ROIs as the parameter to compare different decays, and we calculated the mean value and the associated standard deviation to statistically compare the lifetime decay of different microplastics (resulting in the dataset plotted in figure 4.

CONFOCAL IMAGES: SIZE vs INTENSITY ANALYSIS

The confocal images have been analysed with an ImageJ based macro that finds particles with free shape, size larger than the optical resolution of the microscope, and pixel intensity above a certain threshold. The intensity threshold can be set visually to check that no background pixels are included in the analysis. The results output includes area, minimum, maximum, mean pixel intensities and Intensity integral of the area identified

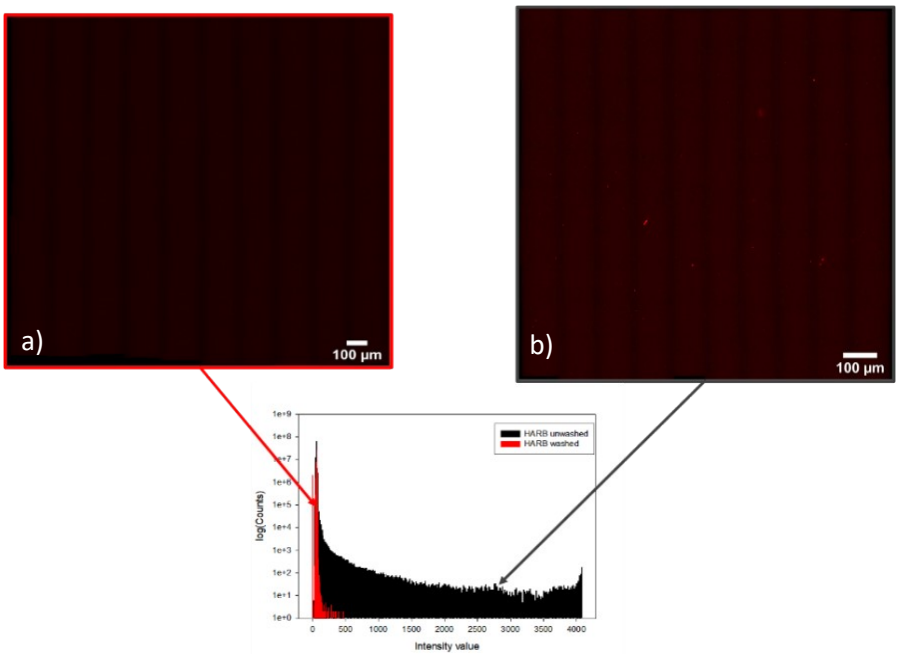

Figure S7 *- Both the images are a multi-frame 10x10 mosaic acquisition. In a) is reported HA-RB subjected to washing process with 60x magnification objective and in b) HA-RB which was not processed with 100x magnification. Same acquisition parameters were used and* images has been acquired between 30 and 50 micron above the surface.

The threshold value is established on a sample of 170 nM HA-RB subjected to washing process in hyaluronan hydrogel used as reference (figure S7). This sample ensures the absence of HA-RB aggregates. From the logarithmic intensity histogram, we chose the intensity threshold to ca. 500 counts, well above background noise (64±12 counts) and slightly varies when we set it for the analysis of different samples. Also, the macro is written to recognize objects above a single pixel size (124 nm) among the selected free shape above the intensity threshold value. These two criteria together with the resolution limit of the instrument (250 nm) show that the analysis result can recognize sub-micron fragment in the MNPs sample (Figure S8). In figure S8 we report the workflow of MNPs image acquisition and analysis.

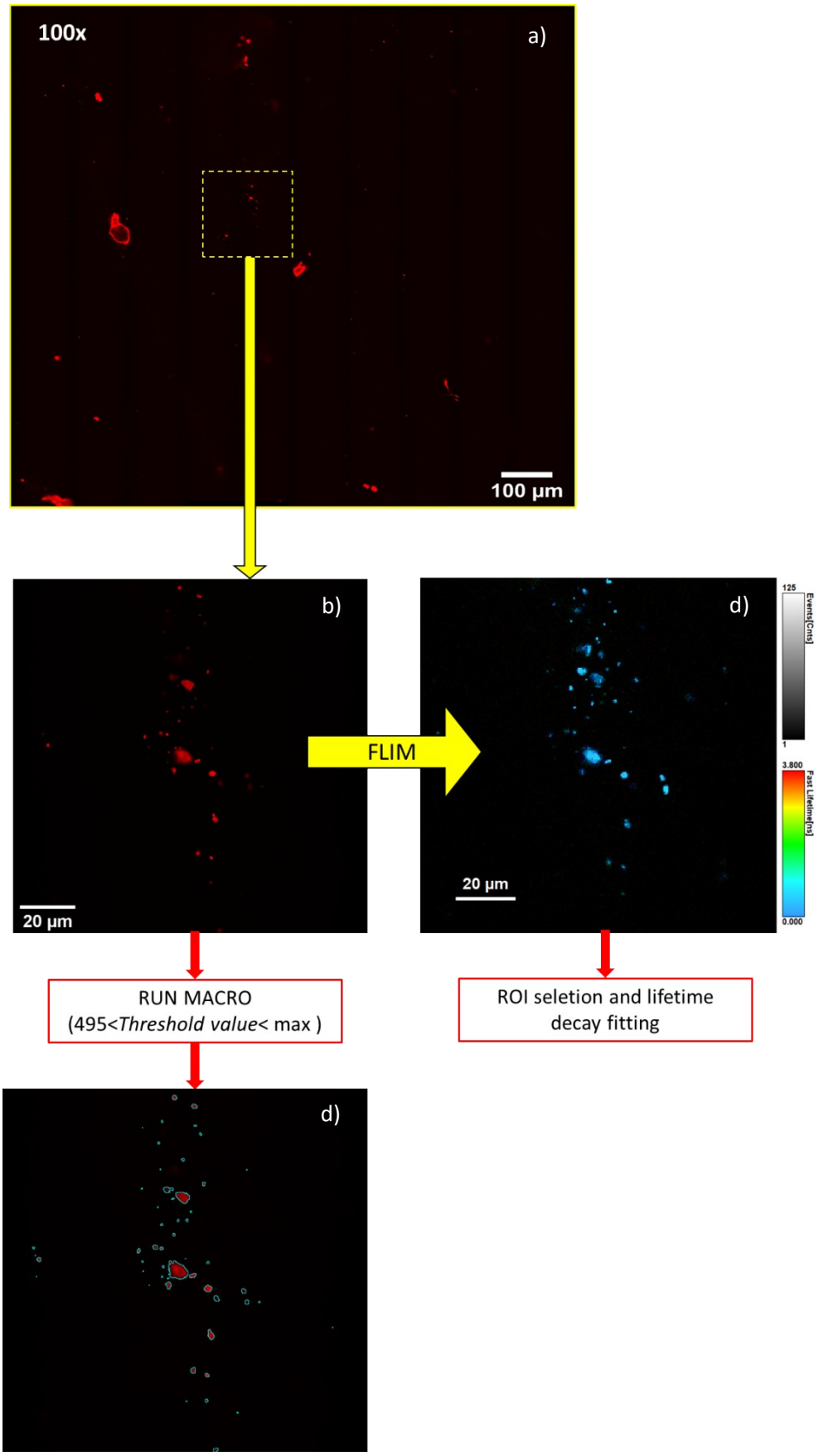
100x
a)
100 µm
b)
20 µm
FLIM
d)
20 µm
125
Events[Cnts]
1
3.800
Fast Lifetime[ns]
0.000
RUN MACRO
(495<*Threshold value*< max)
ROI seletion and lifetime
decay fitting
d)

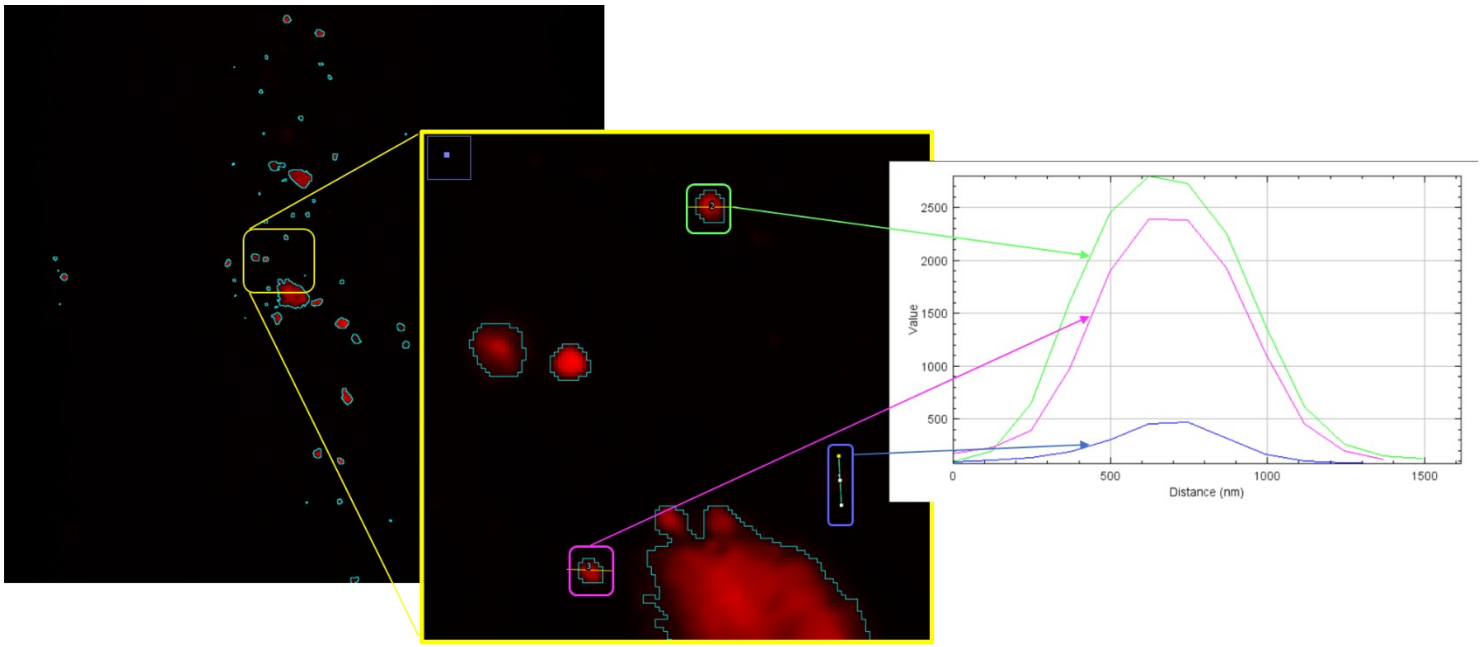

Figure S8 *- Workflow of the acquisition and analysis process for PS microplastic sample. The image a shows a 10x10 mosaic acquisitions with 100x magnification; image b is a single capture and c its corresponding FLIM image; image d shows the resulting area identified by the macro. In the image f there is an enlargement of small fragments identified by the macro routine which intensity profiles (green and pink curve) demonstrate the ability of sub-micron plastics recognition (ca. 500 nm FWHM). The blue curve is associated to a really small fragment whose intensity is equal to the lower value of the threshold and whose dimension is comparable to the microscope resolution limit.*

2.5 Comparison with Rhodamine B molecular dye

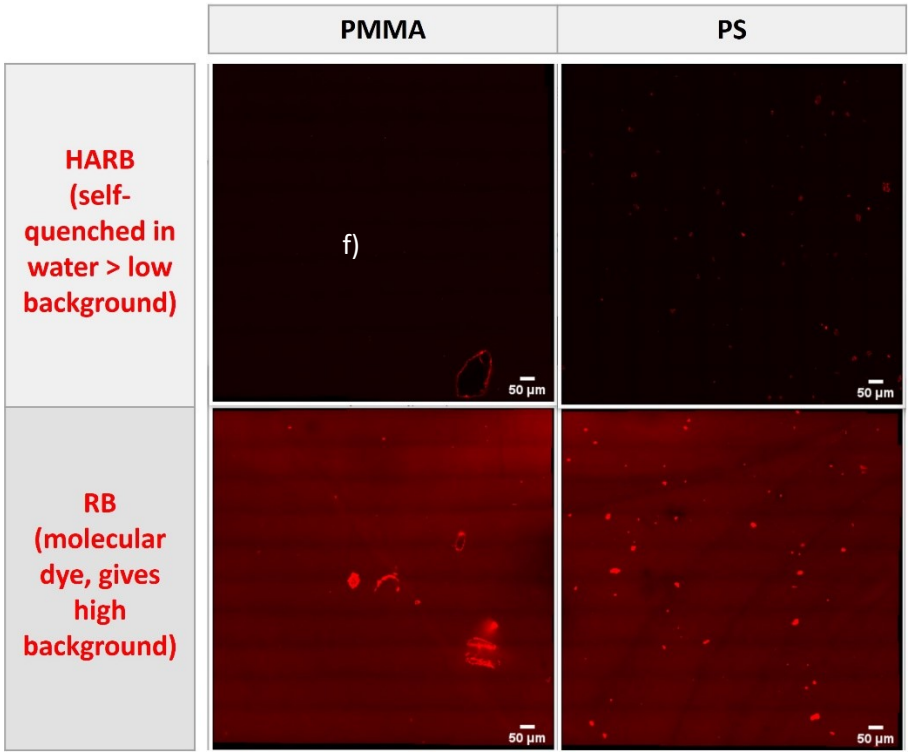

Figure S9 *– Comparison of PMMA (left) and PS (right) MNP staining with HA-RB (top) or molecular dye RB (bottom). Larger fragments are still visible with RB molecular dye but the high background does not allow to visualize the smaller nanoplastic fragments.*

2.6 SEM images of representative MNPs

The SEM micrographs of some representative MNPs samples clearly show, despite the sticking interactions, the presence of fragments of size both above and below one micron., These results confirm the wide size distribution of our samples, already observed by confocal microscopy.

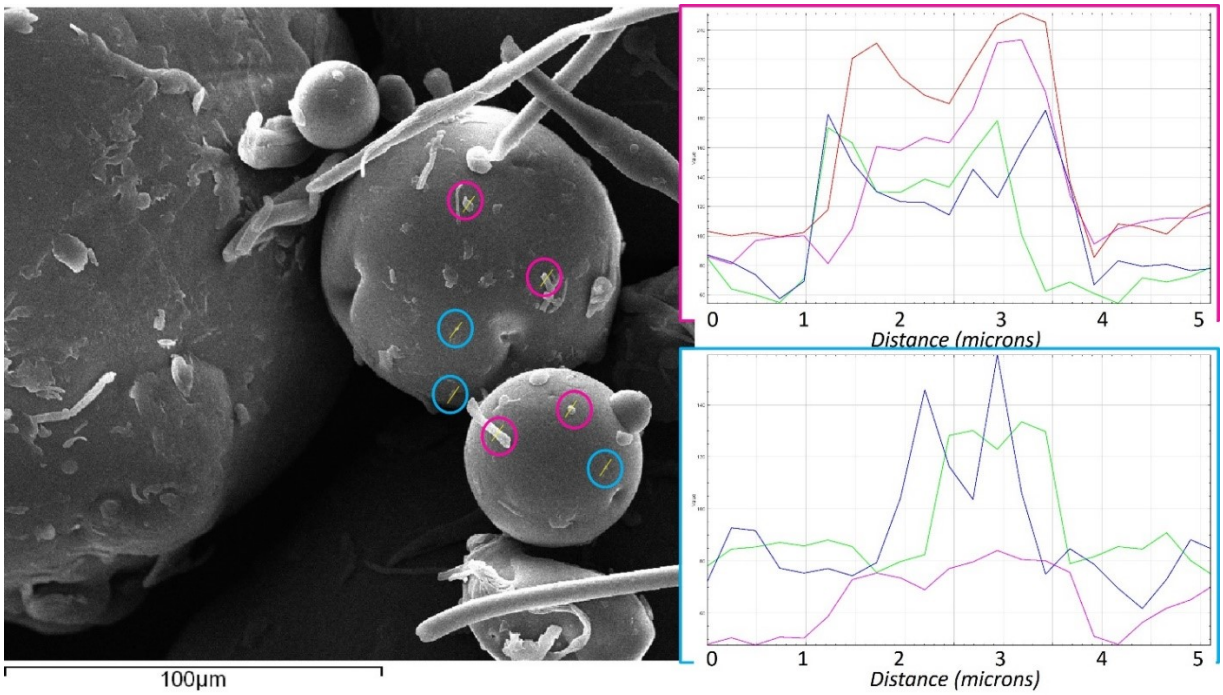

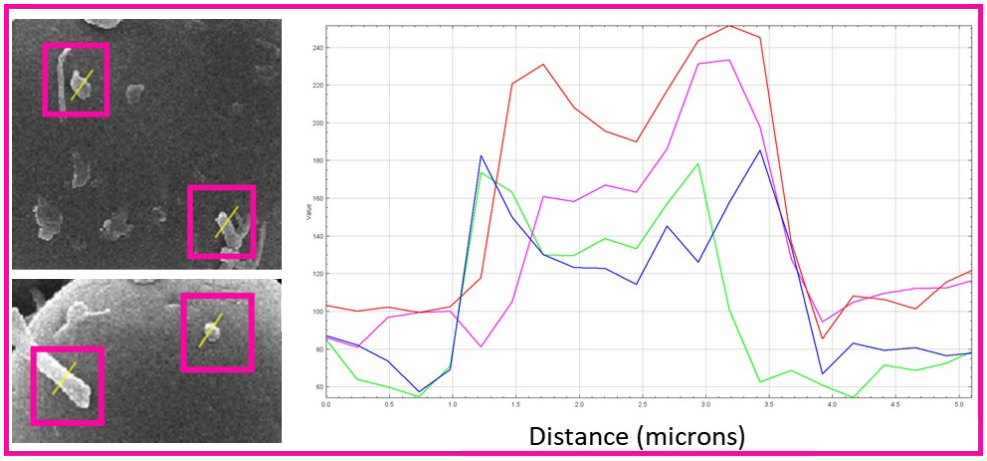

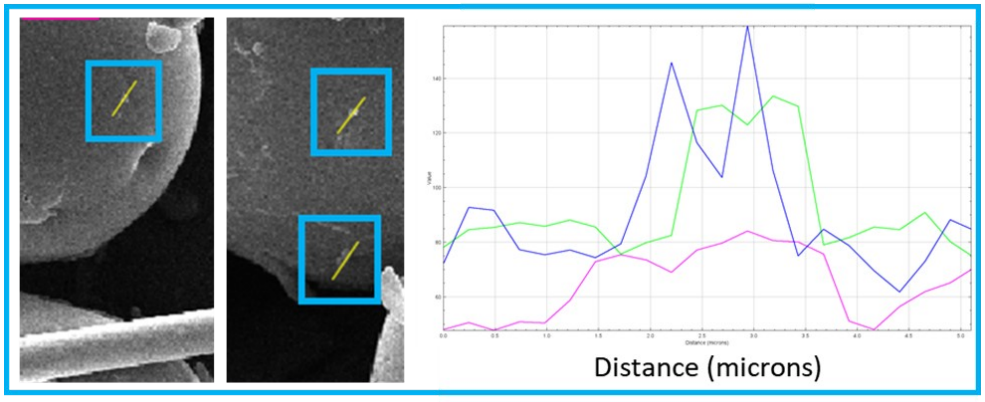

Figure S10 *– SEM micrograph of PE MNPs, with zoomed details of (sub)micrometric fragments.*

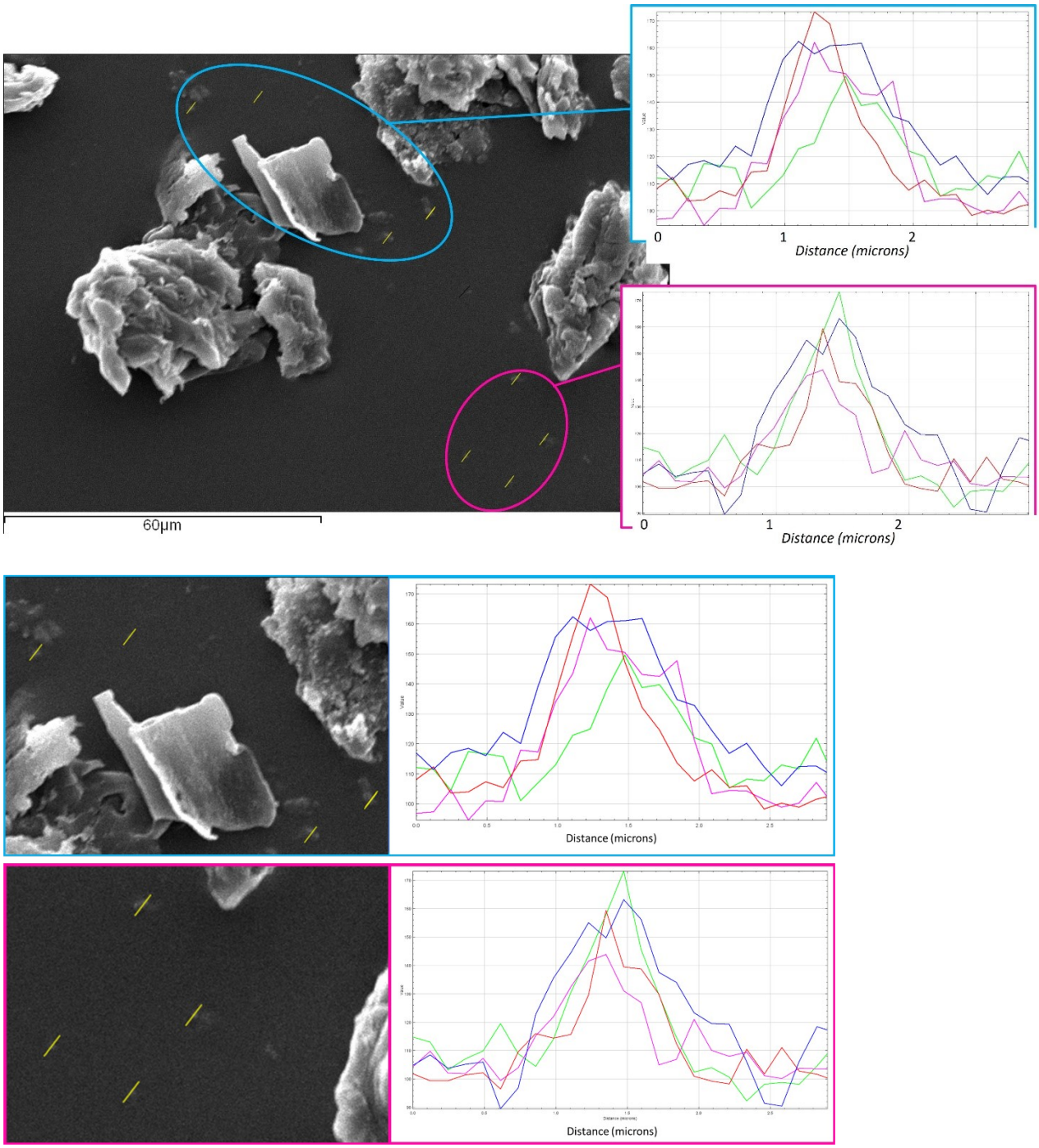

Figure S11 *– SEM micrograph of PMMA MNPs, with zoomed details of (sub)micrometric fragments.*

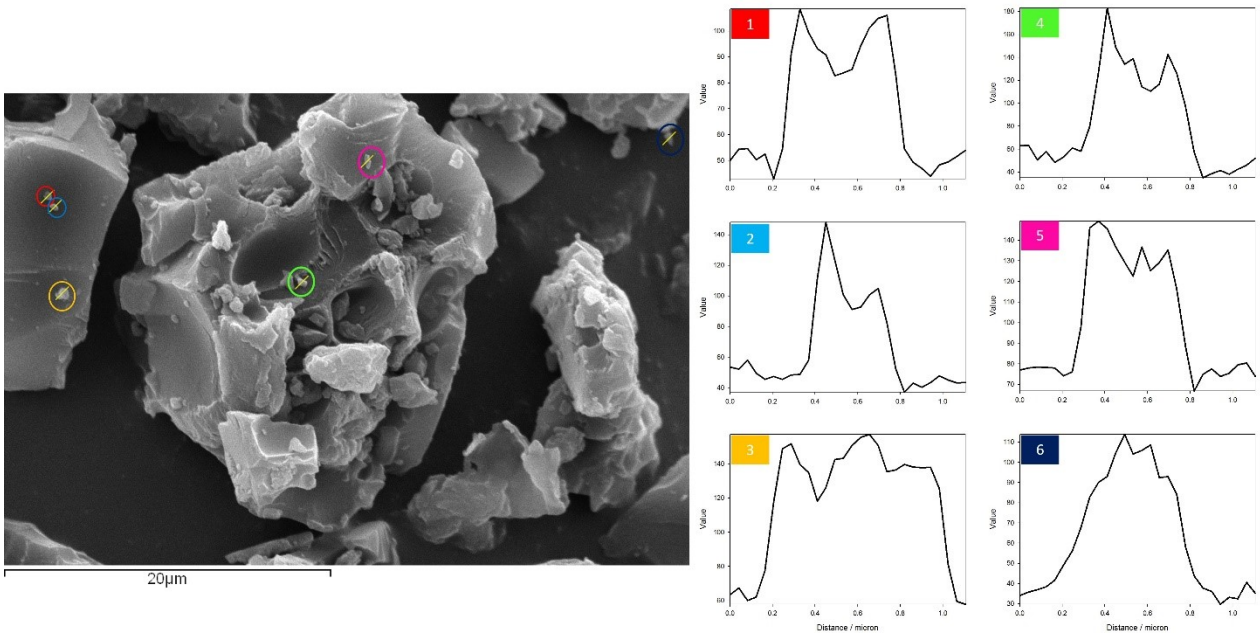

Figure S12 *– SEM micrograph of PS MNPs.*